Geophysical Research Letters

RESEARCH LETTER
10.1029/2019GL082758

# Eddy Compensation Dampens Southern Ocean Sea Surface Temperature Response to Westerly Wind Trends

**Edward W. Doddridge[1], John Marshall[1], Hajoon Song[2], Jean-Michel Campin[1], Maxwell Kelley[3], and Larissa Nazarenko[3]**

[1]Earth, Atmospheric and Planetary Sciences, Massachusetts Institute of Technology, Cambridge, MA, USA, [2]Department of Atmospheric Sciences, Yonsei University, Seoul, South Korea, [3]NASA Goddard Institute for Space Studies, New York, NY, USA

**Key Points:**
- Antarctic circumpolar surface cooling is a robust response to enhanced westerly winds in models and observations
- Mesoscale eddy compensation prevents sustained upwelling of warm water beneath the seasonal ice zone (SIZ)
- Mesoscale eddy transport damps the temperature response of the SIZ to enhanced westerly winds

**Supporting Information:**
- Supporting Information S1

**Correspondence to:**
E. W. Doddridge,
ewd@mit.edu

**Citation:**
Doddridge, E. W., Marshall, J., Song, H., Campin, J.-M., Kelley, M., & Nazarenko, L. S. (2019). Eddy compensation dampens Southern Ocean sea surface temperature response to westerly wind trends. *Geophysical Research Letters*, *46*. https://doi.org/10.1029/2019GL082758

Received 14 MAR 2019
Accepted 30 MAR 2019
Accepted article online 4 APR 2019



**Abstract** Anthropogenic influences have led to a strengthening and poleward shift of westerly winds over the Southern Ocean, especially during austral summer. We use observations, an idealized eddy-resolving ocean sea ice channel model, and a global coupled model to explore the Southern Ocean response to a step change in westerly winds. Previous work hypothesized a two time scale response for sea surface temperature. Initially, Ekman transport cools the surface before sustained upwelling causes warming on decadal time scales. The fast response is robust across our models and the observations: We find Ekman-driven cooling in the mixed layer, mixing-driven warming below the mixed layer, and a small upwelling-driven warming at the temperature inversion. The long-term response is inaccessible from observations. Neither of our models shows a persistent upwelling anomaly, or long-term, upwelling-driven subsurface warming. Mesoscale eddies act to oppose the anomalous wind-driven upwelling, through a process known as eddy compensation, thereby preventing long-term warming.

## 1. Introduction

Over the satellite era, the surface of the Southern Ocean (SO) around Antarctica has been observed to cool, in contrast to much of the rest of the Earth's surface (see, e.g., Armour et al., 2016; Marshall et al., 2015, and references therein). There has also been a striking upward trend in the Southern Annular Mode (SAM) over the same period, especially during the austral summer months of December, January, and February (DJF; Jones et al., 2016; Marshall, 2003). Several modeling studies have suggested that the equilibrium response to a positive shift in the SAM is expected to be a warming at the sea surface and a reduction in sea ice cover (Bitz & Polvani, 2012; Sigmond & Fyfe, 2010, 2013). To reconcile the observed cooling and the modeled equilibrium warming, Ferreira et al. (2015) and Marshall et al. (2014) proposed that the SO responds to a step in the SAM on two distinct time scales: a rapid cooling that occurs within weeks and a slower warming response over the following years to decades. The mechanism behind this two time scale response invokes surface Ekman transports to initially cool the sea surface, with wind-driven upwelling eventually bringing warmer subsurface water, from below the wintertime mixed layer up to the surface in the seasonal ice zone. Other recent studies have suggested additional processes that contribute to the formation of the cold sea surface temperature (SST) anomaly, including atmospheric changes that alter the surface radiation budget (Seviour, Gnanadesikan, et al., 2017) and upwelling of cold water from the previous winter's mixed layer (Purich et al., 2016).

Analysis of the models within the Coupled Model Intercomparison Project Phase 5 (CMIP5) archive reveals substantial agreement on the initial cooling in response to a zonal wind change but a range of long-term responses from continued cooling to rapid warming. The state of affairs is shown in Figure 1a adapted from Kostov et al. (2017, 2018). Kostov et al. (2018) conclude that models that rapidly cross over from cooling to warming in response to a step change in the westerly winds are incompatible with the observed cooling of SST over the past 40 years, given the upward trending SAM over the same period. It should be noted that the historical simulations from the CMIP5 archive models underestimate the trend in westerly winds when compared with observations (Purich et al., 2016). While this should not bias the results of Kostov et al. (2017, 2018), since those analyses present temperature changes per unit change in the SAM, the underestimation

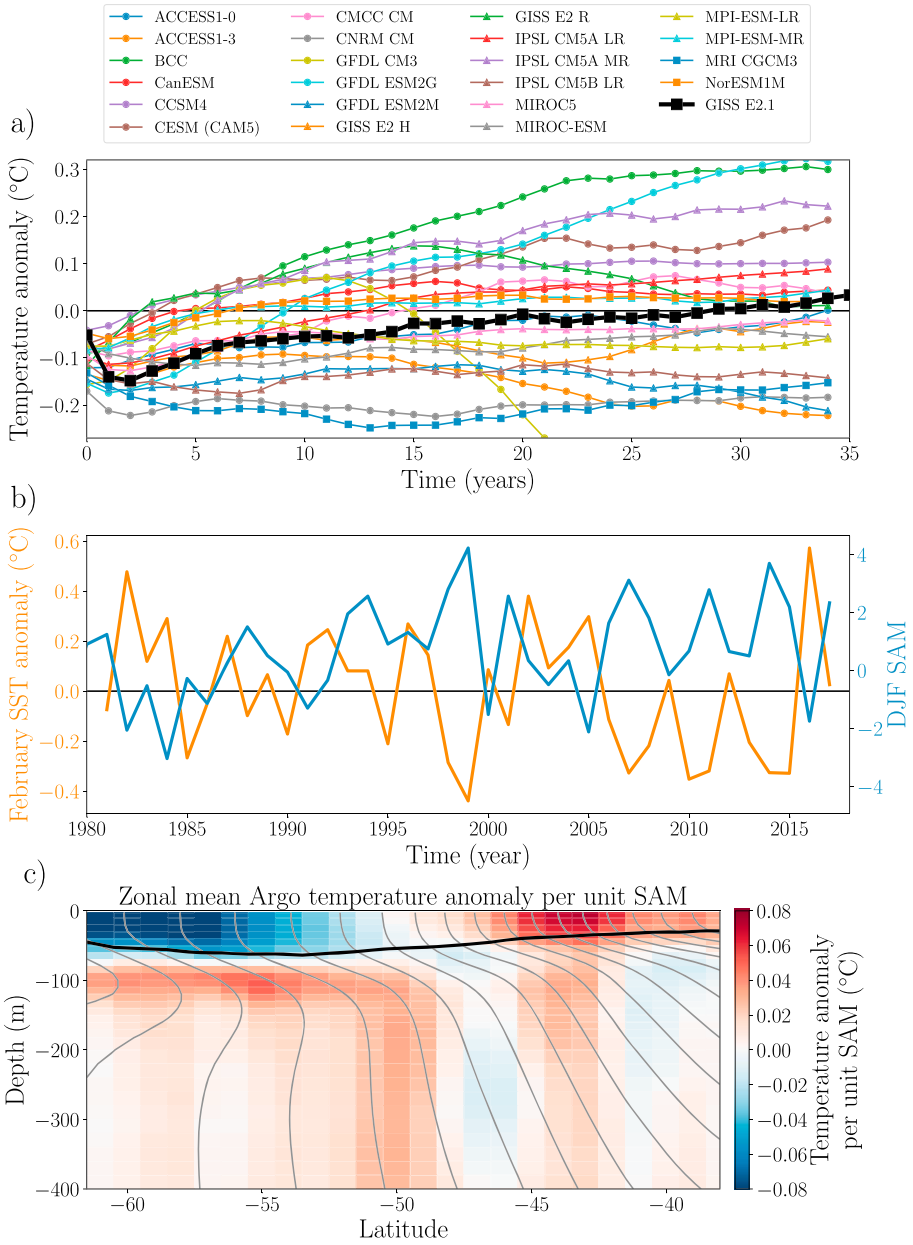


**Figure 1.** (a) Climate response functions of the SST to a one standard deviation step change in the SAM index inferred from various Coupled Model Intercomparison Project Phase 5 models, modified from Kostov et al. (2017). The response of the coupled model used here, developed at GISS and described in the supporting information, is shown by the thick black line. (b) DJF SAM time series from Marshall (2003; blue line, right axis), and February sea surface temperature anomaly between 55°S and 70°S calculated from Reynolds et al. (2002) data (orange line, left axis). (c) Zonal-mean temperature anomaly in February due to a one standard deviation DJF SAM anomaly, estimated from gridded Argo data (Roemmich & Gilson, 2009) and a time series of observed SAM values (Marshall, 2003). The black line is the climatological zonal-mean mixed layer depth from Holte et al. (2017), and the gray contours show the zonal-mean temperature field with a contour interval of 1 °C. DJF = December-January-February; SAM = Southern Annular Mode; SST = sea surface temperature.

of the westerly wind trend likely contributed to the inability of CMIP5 models to capture observed Antarctic sea ice trends (Purich et al., 2016).

The long-term subsurface warming trend discussed by Ferreira et al. (2015) is driven by an intensification of the Deacon Cell due to enhanced westerly winds. However, the expected long-term response of the SO overturning circulation to changes in wind stress is not a sustained strengthening of the Deacon Cell (see, e.g.,

Abernathey et al., 2011; Downes & Hogg, 2013; Gent, 2016; Marshall & Radko, 2003; Viebahn & Eden, 2010). It is instead the residual between an intensification of the wind-driven Deacon Cell and an opposing change in the eddy-driven circulation. The resulting change to the residual overturning circulation is expected to be much smaller than the initial perturbation to the Deacon Cell and to have a different spatial structure. The horizontal resolution of CMIP5 models is too coarse to resolve mesoscale eddies, which must therefore be parameterized (Gent & Mcwilliams, 1990; Gent et al., 1995). Mesoscale eddies are crucial for accurately simulating the behavior of the residual overturning circulation (Abernathey et al., 2011; Downes & Hogg, 2013; Marshall & Radko, 2003) and the strength of the Antarctic Circumpolar Current (Hallberg & Gnanadesikan, 2001, 2006; Hogg & Blundell, 2006; Meredith & Hogg, 2006; Munday et al., 2013; Tansley & Marshall, 2001). Using a mesoscale eddy parameterization coefficient that varies in time and space can substantially improve solutions of non-eddy-resolving ocean models and perhaps how they respond to perturbations (Danabasoglu & Marshall, 2007; Ferreira et al., 2005; Gent, 2016). We might therefore expect that the response of ocean models to changes in the wind depends critically on whether they resolve the eddies responsible for the compensation or, if not, whether they have sufficiently skillful eddy parametrizations to faithfully simulate eddy compensation.

In the following sections we use observations and models to explore the response of the SO to positive SAM perturbations and assess both the short and long time scale responses proposed by Ferreira et al. (2015). The short-term observational response is described in section 2. We then explore the short-term and long-term responses of an idealized eddy-resolving channel model in section 3, before exploring the effect of an ozone-induced SAM perturbation on a global coupled climate model that parameterizes mesoscale eddy transport in section 4. We conclude in section 5 with a discussion of these responses and the consequences of a lack of long-term warming in either model.

## 2. Observed Response of the SO to Positive SAM Perturbations

In the Ferreira et al. (2015) framework, the expected short-term response is a surface cooling and a warming at the temperature inversion, the subsurface region below the seasonal ice zone where $\mathrm{d}T/\mathrm{d}z < 0$, and hence, upwelling leads to warming. The northern edge of this region is clearly visible in the temperature contours in the left-hand side of Figure 1c. Can we detect this signal in observations? We assess the short-term response by comparing the DJF SAM index (Marshall, 2003) and the observed February SST anomaly (averaged between 55°S and 70°S) from Reynolds et al. (2002; Figure 1b). Following Marshall (2003), the DJF SAM values are labeled for the year in which the December occurred. We use February SST anomalies because they exhibit the largest signal related to DJF SAM variability. A linear regression of the DJF SAM values and the February SST yields a strong negative correlation ($R^2 = 0.48$, $p \approx 2 \times 10^{-6}$). This supports the idea that the initial response to a positive SAM perturbation is a surface cooling in the SO close to Antarctica, as has been shown previously in observations (Ciasto & Thompson, 2008; Doddridge & Marshall, 2017) and modeling studies (Ferreira et al., 2015; Seviour et al., 2016, Seviour, Gnanadesikan, et al., 2017, and references therein).

We also use gridded Argo data from 2004 until the present day (Roemmich & Gilson, 2009) to explore the initial, zonal-mean, subsurface response to SAM anomalies. However, there are several observational limitations that should be noted. First, the gridded Argo data set does not extend southward into the seasonal ice zone where the temperature inversion is strongest and where Ferreira et al. (2015) hypothesized that anomalous wind-driven upwelling would lead to subsurface warming. We are therefore unable to assess this subsurface warming, which is a crucial component of the long time scale proposed by Ferreira et al. (2015). Second, the time series is relatively short, which limits the statistical significance of the results. Despite these limitations, a regression analysis of zonal-mean February temperatures from the Argo data set against the DJF SAM time series (Marshall, 2003) reveals a signal of cooling in the mixed layer and warming below related to the positive phase of the SAM index (Figure 1c). The vertical dipole in Figure 1c is centered just beneath the climatological February mixed layer depth from Holte et al. (2017). This is consistent with the strengthened westerly winds enhancing mixing and deepening the mixed layer. During summer there is a shallow mixed layer that is warmer than the cold water beneath. The cold water just below the summertime mixed layer is the remains of the previous wintertime mixed layer. This thermal structure, combined with the enhanced vertical mixing moves heat downward from the surface to just below the zonal-mean mixed layer depth, strengthening the cold anomaly in the mixed layer and warming the fluid below. This warming below the mixed layer is not part of the long-term warming mechanism of Ferreira et al. (2015). Rather,

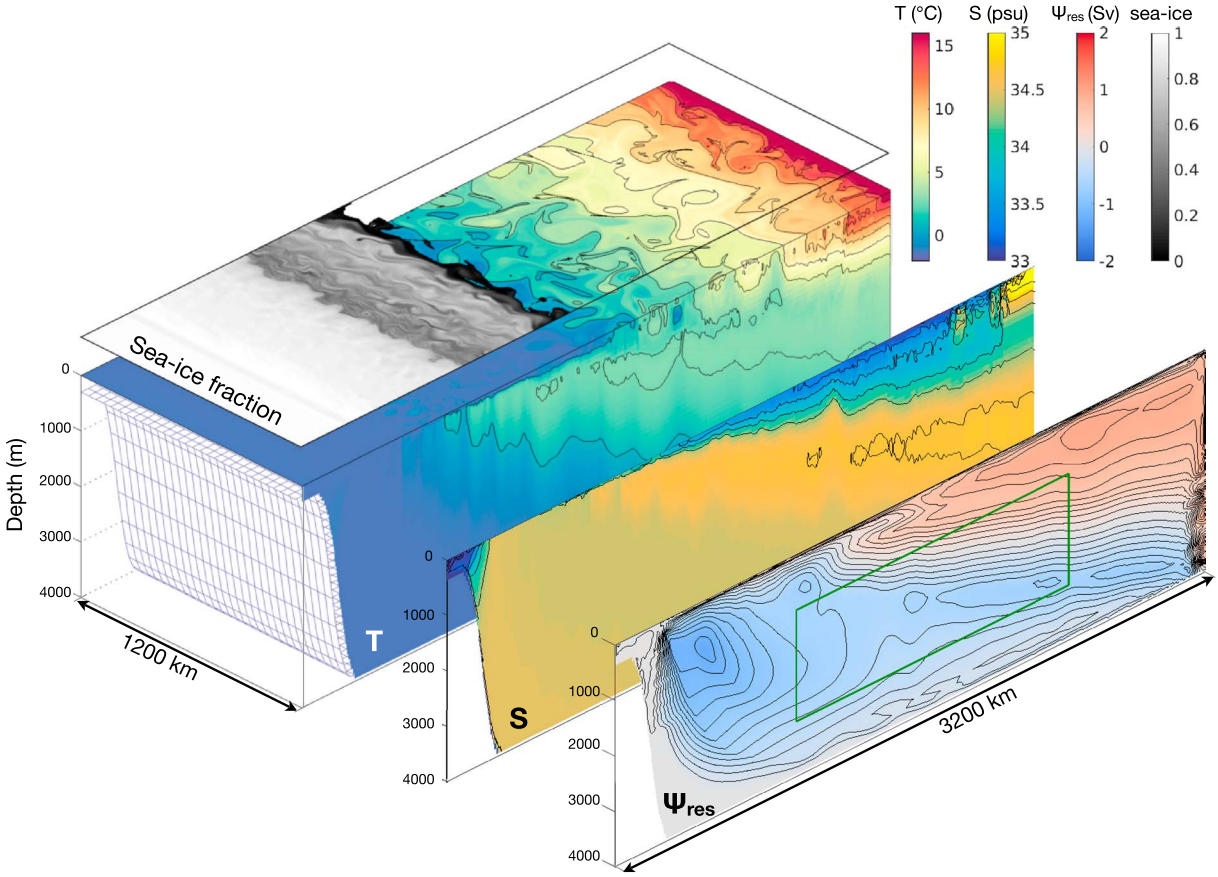


**Figure 2.** Overview of the idealized reentrant eddy-resolving channel control solution showing the instantaneous wintertime sea ice concentration, temperature, and salinity fields, as well as the time-averaged residual overturning circulation. The model is driven by Coordinated Ocean Research Experiments Corrected Normal Year Forcing winds and fluxes. Note the presence of cold, fresh water at the surface in the region of the seasonal ice zone and a pronounced temperature inversion below. The green box indicates the region over which the overturning circulation anomalies are averaged. The region is bounded by $y = 1,000$ km, $y = 2,500$ km, $z = -1,000$ m, and $z = -3,000$ m. Note that the channel is approximately 5% the length of the Antarctic Circumpolar Current, so $\Psi_{\mathrm{res}}$ should be multiplied by ~20 to obtain a global overturning strength.

it is an as yet undescribed feature of the short-term response. In later sections we will see that this vertical dipole is a robust feature across models and show that it is caused by enhanced vertical mixing associated with stronger winds. The Argo data also reveal a summertime reduction in salinity below the zonal-mean mixed layer depth (not shown); this is also consistent with enhanced vertical mixing drawing surface water down from the summertime mixed layer, which is fresher than the water immediately below.

We expect eddy compensation to substantially reduce the anomalous wind-driven upwelling in the seasonal ice zone, thereby diminishing the long-term warming predicted by Ferreira et al. (2015). However, due to the paucity of subsurface measurements in the seasonal ice zone, we are unable to assess the warming anomaly at the temperature inversion or the long-term evolution of zonal-mean temperature anomalies from observations. We therefore turn toward numerical simulations to explore the SO response to enhanced westerly winds.

## 3. Response of an Eddy-Resolving Ocean Sea Ice Channel Model to a Step Change in the Westerly Wind

We use a high-resolution idealized mesoscale eddy-resolving channel model to explore the importance of eddy compensation in the response of the SO to a step change in the westerly wind. An overview of our idealized model is shown in Figure 2, and a more detailed description of the model configuration is given in the supporting information. The domain is a reentrant channel 1,200 km long and 3,200 km wide. There is a continental shelf at the southern edge and a flat bottom elsewhere in the domain. A sponge region at the

northern boundary allows for a meridional overturning circulation. A meridional slice of the monthly mean forcings from the Coordinated Ocean Research Experiments Corrected Normal Year Forcing version 2 data set (Large & Yeager, 2009) at 30°E is used for the surface forcing fields. The Corrected Normal Year Forcing data set represents an idealized annual cycle. As such, our surface forcing contains no interannual variability. The meridional slice is tiled in the zonal direction to cover the entire domain, and hence, there is no zonal variation in the surface forcings. The residual overturning stream function, shown in the outermost panel of Figure 2, exhibits both an upper cell and a lower cell, with the upwelling in the interior occurring along density surfaces, as expected (Marshall & Speer, 2012). The model captures the dynamics of the seasonal ice zone and its interaction with a circumpolar current and its overturning cells.

Once the channel model has reached a statistical equilibrium, we run two ensembles: a control ensemble using the same forcing as the spin-up and a perturbation ensemble in which the zonal wind speed, surface air temperature, and specific humidity are altered in the austral summer months by the addition of a SAM-like anomaly. The perturbation is described in the supporting information. We perturb the surface air temperature and specific humidity so as to prevent unrealistic damping of SST anomalies after the application of the zonal wind perturbation; if these atmospheric fields are left unaltered, then the SST anomaly decays much faster than observational estimates suggest is realistic (Ciasto & Thompson, 2008; Doddridge & Marshall, 2017; Hausmann et al., 2016). We find that six ensemble members are sufficient to obtain a robust response. We define the anomalies as the difference between the perturbation and control ensembles.

Above, we hypothesized that our eddy-resolving model might not exhibit long-term subsurface warming because the eddy-driven overturning circulation would spin up to compensate for the wind-driven change to the residual overturning circulation. The residual overturning circulation can be decomposed into time- and zonal-mean, standing meander, and transient eddy components (Viebahn & Eden, 2012). In models with realistic bathymetry, standing meanders have been shown to play a substantial role in the meridional overturning circulation (Hallberg & Gnanadesikan, 2001). However, the absence of topographic features in our idealized model precludes the presence of standing meanders. The residual meridional overturning circulation can therefore be decomposed into just two terms: the transient eddy component and the Eulerian-mean (time-mean) component. In this decomposition, the Eulerian-mean component is dictated by the surface wind stress (see, e.g., Abernathey et al., 2011) and the transient eddy contribution is diagnosed as the difference between the residual overturning circulation and the Eulerian-mean component. When the SAM perturbation is applied, the surface stress changes, and hence we expect a change in the Eulerian-mean component. Once the perturbation is applied, there is a fast adjustment (less than 1 month), after which the annual-mean Eulerian-mean component of the overturning circulation remains almost constant. Therefore, the subsequent evolution of the residual overturning circulation is due to changes in the transient eddy contribution. Discussing the temporal evolution of the residual overturning circulation is therefore equivalent to discussing changes in the transient eddy contribution. Given that the residual circulation can be directly diagnosed from our simulation, whereas the eddy-induced overturning must be inferred as the difference between the residual and Eulerian-mean circulations, we will discuss the evolution of the residual overturning circulation.

The surface of our idealized channel model initially cools by approximately 0.05 °C (orange line, Figure 3a). While the magnitude of this negative SST anomaly decreases during the 10-year simulation, we do not see sustained long-term warming. The initial cooling is consistent with that found in the CMIP5 models by Kostov et al. (2017). Our model does not exhibit long-term warming at the temperature inversion. The lack of a long-term subsurface warming can be understood by considering the response of the residual overturning stream function. Figure 3a (black line) shows a time series of the anomalous residual overturning circulation averaged over a region below the seasonal ice zone bounded by $y = 1,000$ km, $y = 2,000$ km, $z = -1,000$ m, and $z = -3,000$ m. This region is chosen to provide an estimate of the anomalous upwelling responsible for the long-term warming predicted by Ferreira et al. (2015). Changing the exact region does not qualitatively affect the results, provided that it remains in the seasonal ice zone near the temperature inversion.

The imposed wind anomaly initially increases the upwelling through the temperature inversion (Figures 3a and 3b). However, within 4 years the magnitude of the residual overturning circulation anomaly decreases to approximately 0 (Figure 3a). The evolution of the residual overturning circulation in our idealized channel model is consistent with an initial wind-driven intensification of the Deacon Cell, followed by a spin-up of

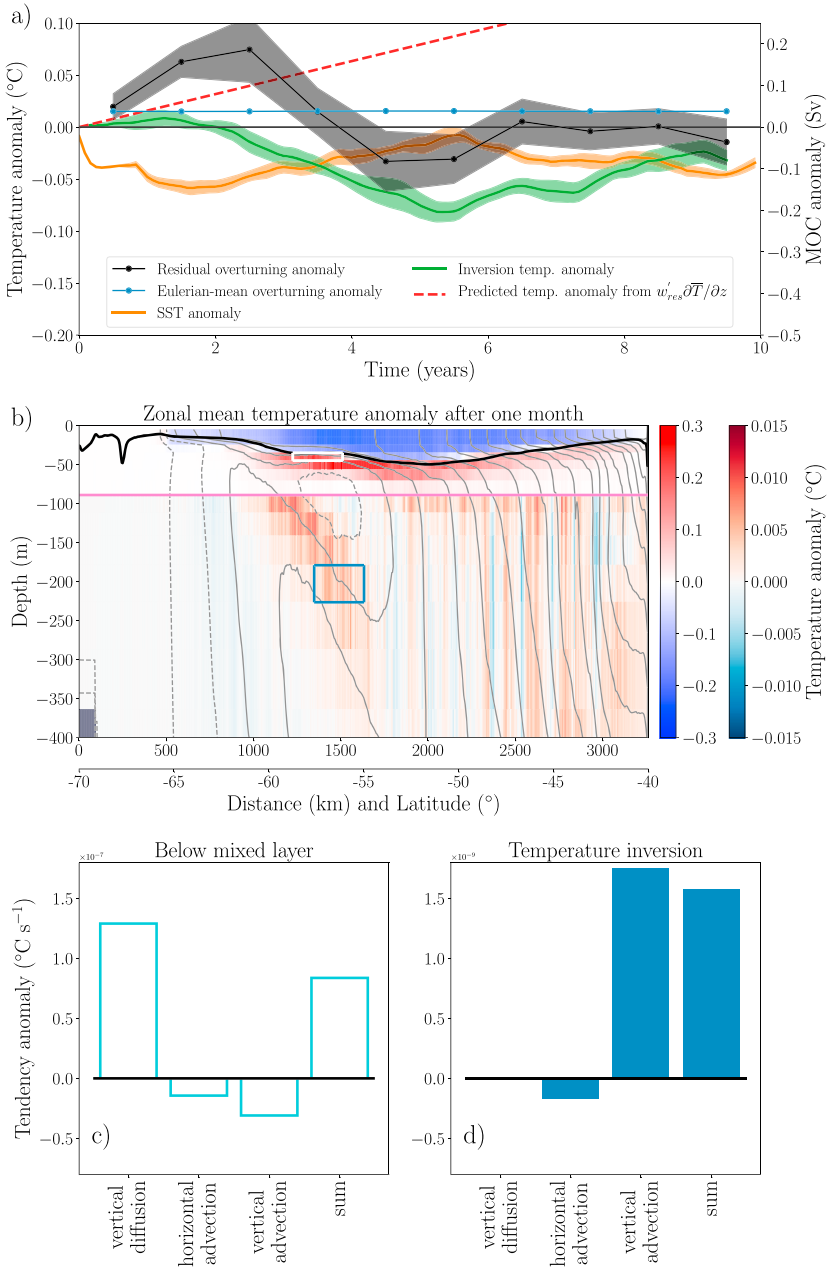


**Figure 3.** (a) Time series of anomalous residual overturning circulation in the channel model (black line, right axis) averaged between $y = 1,000$ and 2,500 km and depths between 1,000 and 3,000 m, Eulerian-mean overturning circulation anomaly (blue line, right axis) averaged between $y = 1,000$ and 2,500 km, the average SST anomaly between $y = 500$ and 2,500 km (orange line), the inversion temperature anomaly at 179-m depth between $y = 1,200$ and 1,600 km (green line), and the predicted inversion temperature anomaly calculated using the average anomalous upwelling and vertical temperature gradient in the first two years (dashed red line). The temperature scale is shown on the left hand axis, and both temperature time series have been smoothed with 12-month running means. Shading represents the standard error of the mean for the ensembles (standard deviation divided by square root of the number of ensemble members). (b) Zonal-mean temperature anomaly (colors) after one month of perturbed forcing. Note the change in color bar at 90 m (horizontal pink line). Light gray contours are the climatological temperature field in February (1 °C contour interval, negative contours dashed), and the thick black line shows the zonal-mean mixed layer depth from the perturbation ensemble calculated using the density-based criterion of Kara et al. (2000) with $\Delta T = 0.8$°C. (c, d) Heat budgets diagnosed one month after the perturbation is applied showing that the anomalous warming below the mixed layer is due to enhanced vertical mixing (panel (c), diagnosed at the white rectangle in (b)), while the warming at the temperature inversion is due to enhanced upwelling (panel (d), diagnosed at the blue rectangle in (b)). The contribution from horizontal mixing is negligible in both regions (see supporting information for the full budget). Note the different vertical scales in (c) and (d). MOC = meridional overturning circulation.

the eddy-driven overturning circulation to oppose the wind-driven change in the residual overturning circulation. It is unclear why the residual overturning anomaly initially overshoots the Eulerian-mean anomaly diagnosed from the surface stress. Six years after the step change is applied, there is no evidence of a net change in the residual overturning stream function. Such a rapid compensation time scale is consistent with previous estimates of the eddy spin-up time scale from observations (Meredith & Hogg, 2006) and idealized models (Screen et al., 2009; Sinha & Abernathey, 2016). Without sustained upwelling through the temperature inversion, the mechanism proposed by Ferreira et al. (2015) cannot lead to long-term warming.

In addition to these anticipated responses, we also find a warm anomaly below the zonal-mean mixed layer depth (Figure 3b). This is very similar to the signal in the observations shown in Figure 1c. Heat budgets averaged in two regions (Figure 3b, white and blue rectangles) indicate that the initial warming in the temperature inversion region is due to enhanced upwelling, while the warming below the mixed layer is due to enhanced vertical mixing (Figures 3c and 3d). The supporting information contains a detailed description of how the heat budgets were computed and a plot with all of the components. The summertime mixed layer is relatively shallow due to the combination of solar heating and weaker wind stress (Panassa et al., 2018), and the mixed layer is warmer than the water directly below. The strengthened westerly winds in our perturbation ensemble drive enhanced near-surface vertical mixing, which acts on this temperature gradient moving heat downward from the surface of the ocean. This means that the enhanced vertical mixing cools the mixed layer and warms the fluid just below the mixed layer. Therefore, the increased vertical mixing strengthens the cold summertime SST anomaly. Both the mixed layer depth and the zonal-mean salinity distribution (not shown) provide further evidence of enhanced vertical mixing. The zonal-mean mixed layer is consistently deeper in the perturbation ensemble than the control ensemble, while the zonal-mean salinity distribution shows an increase in salinity in the mixed layer and a freshening below the mixed layer, consistent with enhanced vertical mixing.

In summary we find that the initial response of the idealized channel model is consistent with the short time scale response proposed by Ferreira et al. (2015): We see a cooling at the surface driven by horizontal Ekman transport and a slight warming at the level of the temperature inversion due to enhanced upwelling. However, eddy compensation damps the anomalous upwelling within a few years. Because the eddy-induced overturning circulation spins up to oppose the wind-driven anomalous upwelling, we do not observe the long-term subsurface warming hypothesized by Ferreira et al. (2015).

## 4. Response to a Step Ozone Perturbation in a Comprehensive Coupled Climate Model

The results from our idealized channel model are instructive, but the model uses a simplified domain and imposed atmospheric forcings. Due to its flat bottom, our channel model cannot represent flow-topography interactions and standing meanders, which have been shown to play an important role in tracer transport (Bryan et al., 2014; Spence et al., 2012; Tamsitt et al., 2017) and to contribute to eddy compensation (Dufour et al., 2012; Zika et al., 2013). To assess whether the results presented above are predicated on the simplified nature of the channel model, we now analyze an ensemble of coupled global simulations. In this section we present results from simulations using the most recent National Aeronautics and Space Administration GISS coupled climate model, Model E2.1. Because these are global coupled simulations, the horizontal resolution is much coarser than the idealized model; the oceanic component of the global model uses a $1° \times 1.25°$ latitude-longitude grid. As such, these results come with the caveat that mesoscale eddy transport is parameterized rather than explicitly resolved. From a long equilibrium preindustrial control, we spawn perturbation experiments in which a seasonal hole in the stratospheric Antarctic ozone distribution is imposed to mimic conditions in the 1990s. Eight ensemble members are averaged to reduce the impact of internal variability. Once again, we define the anomalies as the difference between the control ensemble and the perturbation ensemble. As a result of the ozone perturbation, the Southern Hemisphere westerlies shift poleward, simultaneously enhancing summertime westerly winds around Antarctica and reducing them further north (Figure 4a). This enhancement of westerly winds during the austral summer is a well-known consequence of stratospheric ozone depletion (see, e.g., Gerber & Son, 2014; Polvani et al., 2011; Seviour, Waugh, et al., 2017).

The strengthened surface westerly winds initially cause cold SST anomalies through enhanced equatorward Ekman transport (Figure 4b, orange line). We also observe anomalous upwelling due to a Deacon Cell-like

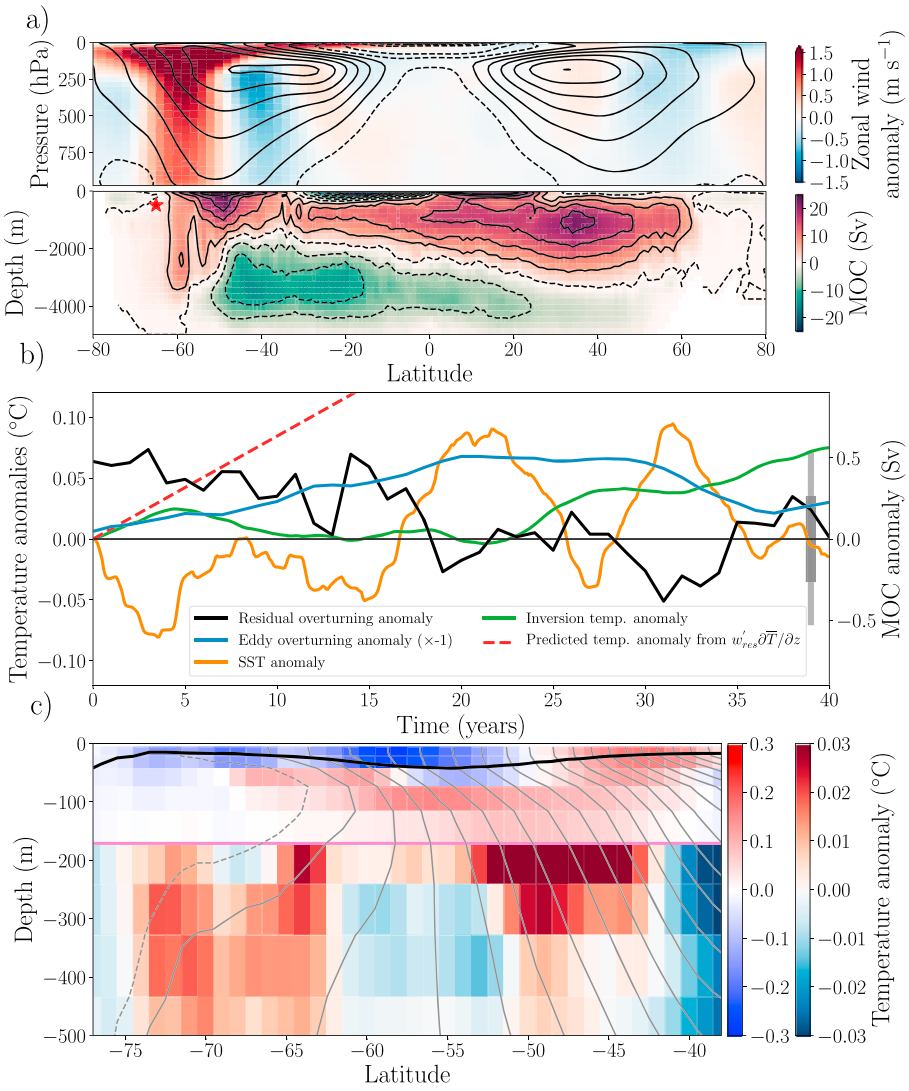


**Figure 4.** (a) Upper panel: time- and zonal-mean zonal wind in January from the 60-year-long control ensemble (contours with 5-m/s contour interval, zero, and negative contours dashed) and climatological zonal-mean zonal wind anomalies in January due to ozone perturbation (colors). Lower panel: time-averaged residual overturning circulation from the control simulation (contours have a 5-Sv contour interval, zero, and negative contours are dashed). (b) Time series of the anomalous residual overturning circulation (black line, right axis) and the sum of the resolved and parameterized eddy-driven overturning circulation (blue line, right axis) extracted at the red star in (a) located at 65°S and 492-m depth. Time series of the anomalous temperature at the temperature inversion (73–63°S, 328-m depth, green line), the SST anomaly (70–55°S, orange line), and the anticipated temperature anomaly at the inversion calculated from the anomalous upwelling averaged over the first 10 years of the perturbation experiment and the climatological vertical temperature gradient from the control ensemble (dashed red line), with temperature scale shown on the left hand axis. All lines represent ensemble means and have been smoothed with a 5-year running mean. The thin and thick gray vertical shaded regions show the variability of the control ensemble SST and represent $1\sigma$ and $2\sigma$, respectively. (c) Zonal-mean temperature anomaly (colors) in February of the second year of the simulation and the climatological temperature in February from the control ensemble (gray contours, contour interval 1 °C, negative contours dashed). The vertical dipole of cooling and warming centered on the mixed layer depth can be clearly seen, as can the warming at the temperature inversion. The zonal-mean mixed layer depth from the perturbation ensemble is shown by the black line. Note the change in color scale either side of the horizontal pink line at 171-m depth. MOC = meridional overturning circulation; SST = sea surface temperature.

perturbation to the residual overturning circulation (Figure 4b, black line). After 20 years the initial anomalous residual overturning circulation has been almost completely opposed by the sum of the resolved and parameterized eddy-induced overturning circulations. Although the time scale of eddy compensation is much longer in this model than the channel model, we again find a substantial reduction in the anomalous wind-driven upwelling and no evidence of long-term upwelling-induced subsurface warming at the temperature inversion. In the first 5 years of the simulation we see both anomalous upwelling (the residual overturning anomaly, black line in Figure 4b is positive) and warming at the inversion (green line, Figure 4b). Between years 5 and 20 the residual overturning anomaly decreases to 0 and there is no additional warming at the temperature inversion. Beyond year 20, the temperature anomaly at the inversion does increase, but anomalous upwelling cannot be the causal mechanism because the overturning anomaly is small by this time (Figure 4b, black line). At the same time oscillations in the SST and overturning appear which we attribute to internal variability, the amplitude of which is indicated by the vertical gray bar in Figure 4b. The oscillations in SST and overturning anomalies appear to show some weak correlation.

The vertical structure of the temperature anomaly is characterized by a cooling-warming dipole centered on the mixed layer depth and a weak warming at the temperature inversion (Figure 4c). This pattern is strikingly similar to that found in the channel model (Figure 3b) and in the observations (Figure 1c), and the mechanisms causing the warming are the same as those diagnosed in the channel model (see supporting information for a heat budget).

The initial SST response reveals a cooling, but the long-term evolution of SST is less clear. Despite analyzing an ensemble of simulations, the presence of internal variability with a magnitude of approximately 0.1 °C from year 15 onward makes it difficult to identify whether a warming trend is present in the latter part of the time series. Taking an average of the SST anomaly between years 20 and 40 shows a small warming, consistent with the climate response function shown in Figure 1a. Despite the variability in the latter part of the time series, the lack of substantial warming at the temperature inversion during the time period with anomalous upwelling rules out the mechanism proposed by Ferreira et al. (2015) as a source of any long-term warming in this model.

We conclude that the second time scale of the two time scale response proposed by Ferreira et al. (2015) is very long in the GISS model and that the warming is weak. Taking an average of the SST perturbation in the final decades of the simulation reveals only a moderate warming, and there is no evidence of a strong warming trend by this time. The SST response in our perturbation experiment is remarkably consistent with the climate response function deduced by lagged regression between SAM and SST from a long control run of the GISS E2.1 model (Figure 1a, black line) that just barely crosses over into warming after 35 years.

## 5. Discussion and Conclusions

Ferreira et al. (2015) proposed a two time scale mechanism drawing together observational evidence that strengthening westerly winds were associated with a cooling of the sea surface and an expansion of sea ice, and modeling evidence that suggested stratospheric ozone depletion would eventually lead to warmer SSTs and a loss of sea ice. However, the mechanism proposed by Ferreira et al. (2015) relies on a persistent intensification of the Deacon Cell and a growing subsurface temperature anomaly that is eventually entrained into the mixed layer thereby warming the sea surface. While we are unable to address the long-term changes from observations, we do not find this mechanism at work in either of our numerical experiments. Instead, we see a transient intensification of the Deacon Cell, which then fades and does not lead to subsurface warming in the seasonal ice zone. While atmospheric processes may also be important, as suggested by Seviour, Gnanadesikan, et al. (2017), the mechanism we have focused on here is an oceanic one, and we find no evidence of a subsurface warming driven by anomalous upwelling. Instead, we find that anomalous upwelling fades over time.

The initial response to strengthened westerly winds is consistent between the observations, an idealized eddying ocean sea ice model, and a global coupled model. In each of these cases we observe a vertical cooling-warming dipole centered on the zonal-mean mixed layer depth. The warming just below the mixed layer is driven by anomalous vertical mixing caused by the strengthened westerly winds. This near-surface mixing signal is unrelated to the purely advective mechanism proposed by Ferreira et al. (2015). The observations and the coupled model also show a warming to the north, in the region where the westerly winds weaken due to a poleward shift in the atmospheric jet.

The long time scale is inaccessible from observations but can be addressed in our models. In both models, we initially find a small warming at the temperature inversion in the seasonal ice zone. However, this small warming anomaly fades rapidly (within 2 years in the channel model and 10 years in the fully coupled model). Furthermore, the models do not exhibit the persistent and substantial anomalous upwelling required by the Ferreira et al. (2015) mechanism. In our idealized channel model, the lack of persistent and substantial upwelling is due to a change in the eddy-driven overturning circulation that compensates for the altered wind-driven overturning. This is eddy compensation (see, e.g., Abernathey et al., 2011; Downes & Hogg, 2013; Gent, 2016; Viebahn & Eden, 2010).

Because the GISS model is a complex global coupled model, the lack of substantial subsurface warming in the first 20 years could be due to many different physical processes. We can, however, say that the anomalous overturning circulation induced by the ozone hole decays away over time and does not cause subsurface warming in the seasonal ice zone. The positive subsurface temperature anomaly in the GISS model from year 20 onward cannot be related to the upwelling mechanism proposed by Ferreira et al. (2015) since the overturning anomaly is small by that time. The SST response clearly shows an initial cooling, consistent with the two time scale mechanism of Ferreira et al. (2015). However, the predicted long-term increase in SST does not materialize. While it is possible that the oscillations which appear after year 15 mask a weak warming trend, the lack of subsurface warming in the preceding years rules out the two time scale mechanism proposed by Ferreira et al. (2015).

Our idealized channel model has a flat bottom apart from a continental shelf at the southern edge of the domain, which precludes the development of standing meanders in our circumpolar current. In models that contain standing meanders, these meanders have been shown to contribute substantially to eddy compensation (Dufour et al., 2012; Zika et al., 2013), tracer transport, and upwelling (Bryan et al., 2014; Spence et al., 2012; Tamsitt et al., 2017). The lack of standing meanders in our idealized channel potentially restricts the dynamics in such a way that artificially alters our results. For this reason we also analyzed a global coupled model that uses realistic bathymetry and therefore supports standing meanders. The results from our coupled model are very similar to those of our idealized channel model; we find an initial wind-driven upwelling anomaly, which then decreases as the parameterized eddy compensation occurs. In neither model can we identify the persistent upwelling-driven subsurface warming predicted by Ferreira et al. (2015).

Both our coupled ensemble and the ensembles presented by Ferreira et al. (2015) use a Gent-McWilliams style eddy parameterization (Gent & Mcwilliams, 1990; Gent et al., 1995) that relates the slope of the isopycnals to the strength of the eddy-induced overturning circulation using the eddy diffusivity, $\kappa_{GM}$. In the simplest parameterizations, where $\kappa_{GM}$ does not depend on the isopycnal slope, the strength of the eddy-induced circulation is directly proportional to the isopycnal slope. The simulations performed by Ferreira et al. (2015) used either a constant for $\kappa_{GM}$ (MITgcm ensemble), or a vertically variable $\kappa_{GM}$ following Ferreira et al. (2005) and Danabasoglu and Marshall (2007) that depends on the local stratification (CCSM3.5 ensemble). In neither case does the value of $\kappa_{GM}$ depend on the isopycnal slope. The parameterization used by GISS Model E2.1 dynamically assigns $\kappa_{GM}$ based on the flow and isopycnal slope. This means that the strength of the eddy-induced overturning circulation is proportional to the isopycnal slope raised to the power $n$, where $2 \leq n \leq 3$ (see supporting information for details of the parameterization). Since the eddy-induced overturning depends on the isopycnal slope raised to some power, small changes in the slope produce relatively large changes in the eddy-induced overturning circulation. This sensitivity helps prevent wind perturbations from causing large changes to the isopycnal slopes and may explain why our coupled simulations did not show the warming predicted by Ferreira et al. (2015).

Our results contrast with those of Bitz and Polvani (2012) who found that their eddy-resolving coupled climate model did warm in response to an ozone perturbation. But Figure 3 in Bitz and Polvani (2012) shows that the zonal-mean ocean warming does not occur near the temperature inversion. Rather, they find warming further north and attribute it to anomalous downwelling. However, it should be noted that their Figure 4 shows the Eulerian-mean overturning, rather than the more pertinent residual overturning circulation (Marshall & Radko, 2003).

Finally, Kostov et al. (2018) show that CMIP5 models have a wide range of responses to a step change in the SAM. They conclude that models that exhibit strong warming are incompatible with the observational record. Furthermore, long-term warming caused by a persistent intensification of the Deacon Cell, as hypothesized by Ferreira et al. (2015), is inconsistent with our current understanding of SO dynamics. Here

we have presented two numerical simulations that do not exhibit long-term warming and shown that this is related to an eddy-driven reduction in the anomalous wind-driven upwelling. This suggests that the second time scale from Ferreira et al. (2015) is very long and that the resultant warming is weak. Our results lend support to the conclusions of Kostov et al. (2018) and identify an important ocean mechanism at work that damps the temperature response of the seasonal ice zone to anomalous winds.

**Acknowledgments**
E. W. D. acknowledges support from the NSF's FESD program. J. M. acknowledges support from the MIT-GISS collaborative agreement and the NSF Polar Antarctic Program. H. S. was supported (in part) by the Yonsei University Future-leading Research Initiative of 2018 (2018-22-0053). We gratefully acknowledge Hannah Zanowski, David Ferreira, and an anonymous reviewer for their insightful comments that substantially improved this manuscript. Climate modeling at NASA-GISS is supported by the NASA Modeling, Analysis, and Prediction program. Computational resources for the E2.1 simulations in this study were provided by the NASA High-End Computing Program through the NASA Center for Climate Simulation (NCCS) at Goddard Space Flight Center. We are grateful to Douglas Kinnison for assistance with the ozone perturbation for the GISS simulations. The National Center for Atmospheric Research (NCAR) is sponsored by the U.S. National Science Foundation (NSF). WACCM is a component of NCAR's Community Earth System Model (CESM), which is supported by the NSF and the Office of Science of the U.S. Department of Energy. Computing resources were provided by NCAR's Climate Simulation Laboratory, sponsored by NSF and other agencies. This research was enabled by the computational and storage resources of NCAR's Computational and Information Systems Laboratory (CISL). The WACCM model output and data used in this paper are listed in the references or available from the NCAR Earth System Grid. The numerical simulations presented in this study relied on numerous contributions to the literature that are detailed in the supporting information (Adcroft et al., 1997; Dee et al., 2011; Garcia et al., 2007, 2017; Gaspar et al., 1990; Gent & Mcwilliams, 1990; Gent et al., 1995; Hunke & Dukowicz, 1997; Kinnison et al., 2007; Kunz et al., 2011; Lamarque et al., 2012; Large & Pond, 1982; Large & Yeager, 2009; Large et al., 1994; Lin, 2004; Locarnini et al., 2013; Losch et al., 2010; Marsh et al., 2013; Marshall, Hill, et al., 1997, 1998, Marshall, Adcroft, et al., 1997; Morgenstern et al., 2017; Neale et al., 2013; Redi, 1982; Rienecker et al., 2011; Schmidt et al., 2014; Solomon et al., 2015; Tilmes et al., 2016; Visbeck et al., 1997; Winton, 2000; Zweng et al., 2013).

## References

Abernathey, R., Marshall, J. C., & Ferreira, D. (2011). The dependence of Southern Ocean Meridional Overturning on wind stress. *Journal of Physical Oceanography*, *41*(12), 2261–2278. https://doi.org/10.1175/JPO-D-11-023.1

Adcroft, A. J., Hill, C., & Marshall, J. C. (1997). Representation of topography by shaved cells in a height coordinate ocean model. *Monthly Weather Review*, *125*, 2293–2315. https://doi.org/10.1175/1520-0493(1997)125<2293:ROTBSC>2.0.CO;2

Armour, K. C., Marshall, J. C., Scott, J. R., Donohoe, A., & Newsom, E. R. (2016). Southern Ocean warming delayed by circumpolar upwelling and equatorward transport. *Nature Geoscience*, *9*(7), 549–554. https://doi.org/10.1038/ngeo2731

Bitz, C. M., & Polvani, L. M. (2012). Antarctic climate response to stratospheric ozone depletion in a fine resolution ocean climate model. *Geophysical Research Letters*, *39*, L20705. https://doi.org/10.1029/2012GL053393

Bryan, F. O., Gent, P. R., & Tomas, R. (2014). Can Southern Ocean eddy effects be parameterized in climate models? *Journal of Climate*, *27*(1), 411–425. https://doi.org/10.1175/JCLI-D-12-00759.1

Ciasto, L. M., & Thompson, D. W. J. (2008). Observations of large-scale ocean-atmosphere interaction in the Southern Hemisphere. *Journal of Climate*, *21*(6), 1244–1259. https://doi.org/10.1175/2007JCLI1809.1

Danabasoglu, G., & Marshall, J. C. (2007). Effects of vertical variations of thickness diffusivity in an ocean general circulation model. *Ocean Modelling*, *18*(2), 122–141. https://doi.org/10.1016/j.ocemod.2007.03.006

Dee, D. P., Uppala, S. M., Simmons, A. J., Berrisford, P., Poli, P., Kobayashi, S., et al. (2011). The ERA-Interim reanalysis: Configuration and performance of the data assimilation system. *Quarterly Journal of the Royal Meteorological Society*, *137*(656), 553–597. https://doi.org/10.1002/qj.828

Doddridge, E. W., & Marshall, J. C. (2017). Modulation of the seasonal cycle of Antarctic sea ice extent related to the Southern Annular Mode. *Geophysical Research Letters*, *44*, 9761–9768. https://doi.org/10.1002/2017GL074319

Downes, S. M., & Hogg, A. M. C. C. (2013). Southern Ocean circulation and eddy compensation in CMIP5 models. *Journal of Climate*, *26*(18), 7198–7220. https://doi.org/10.1175/JCLI-D-12-00504.1

Dufour, C. O., Le Sommer, J., Zika, J. D., Gehlen, M., Orr, J. C., Mathiot, P., & Barnier, B. (2012). Standing and transient eddies in the response of the Southern Ocean Meridional Overturning to the Southern Annular Mode. *Journal of Climate*, *25*(20), 6958–6974. https://doi.org/10.1175/JCLI-D-11-00309.1

Ferreira, D., Marshall, J. C., Bitz, C. M., Solomon, S., & Plumb, A. (2015). Antarctic ocean and sea ice response to ozone depletion: A two-time-scale problem. *Journal of Climate*, *28*(3), 1206–1226. https://doi.org/10.1175/JCLI-D-14-00313.1

Ferreira, D., Marshall, J. C., & Heimbach, P. (2005). Estimating eddy stresses by fitting dynamics to observations using a residual-mean ocean circulation model and its adjoint. *Journal of Physical Oceanography*, *35*(10), 1891–1910. https://doi.org/10.1175/JPO2785.1

Garcia, R. R., Marsh, D. R., Kinnison, D. E., Boville, B. A., & Sassi, F. (2007). Simulation of secular trends in the middle atmosphere, 1950–2003. *Journal of Geophysical Research*, *112*, D09301. https://doi.org/10.1029/2006JD007485

Garcia, R. R., Smith, A. K., Kinnison, D. E., de la Cámara, Á., & Murphy, D. J. (2017). Modification of the gravity wave parameterization in the Whole Atmosphere Community Climate Model: Motivation and results. *Journal of the Atmospheric Sciences*, *74*(1), 275–291. https://doi.org/10.1175/JAS-D-16-0104.1

Gaspar, P., Grégoris, Y., & Lefevre, J.-M. (1990). A simple eddy kinetic energy model for simulations of the oceanic vertical mixing: Tests at station Papa and long-term upper ocean study site. *Journal of Geophysical Research*, *95*(C9), 16,179–16,193. https://doi.org/10.1029/JC095iC09p16179

Gent, P. R. (2016). Effects of Southern Hemisphere wind changes on the meridional overturning circulation in ocean models. *Annual Review of Marine Science*, *8*(1), 79–94. https://doi.org/10.1146/annurev-marine-122414-033929

Gent, P. R., & Mcwilliams, J. C. (1990). Isopycnal mixing in ocean circulation models. *Journal of Physical Oceanography*, *20*(1), 150–155. https://doi.org/10.1175/1520-0485(1990)020<0150:IMIOCM>2.0.CO;2

Gent, P. R., Willebrand, J., McDougall, T. J., & McWilliams, J. C. (1995). Parameterizing eddy-induced tracer transports in ocean circulation models. *Journal of Physical Oceanography*, *25*(4), 463–474. https://doi.org/10.1175/1520-0485(1995)025<0463:PEITTI>2.0.CO;2

Gerber, E. P., & Son, S. W. (2014). Quantifying the summertime response of the Austral jet stream and Hadley cell to stratospheric ozone and greenhouse gases. *Journal of Climate*, *27*(14), 5538–5559. https://doi.org/10.1175/JCLI-D-13-00539.1

Hallberg, R., & Gnanadesikan, A. (2001). An exploration of the role of transient eddies in determining the transport of a zonally reentrant current. *Journal of Physical Oceanography*, *31*(11), 3312–3330. https://doi.org/10.1175/1520-0485(2001)031<3312:AEOTRO>2.0.CO;2

Hallberg, R., & Gnanadesikan, A. (2006). The role of eddies in determining the structure and response of the wind-driven Southern Hemisphere overturning: Results from the Modeling Eddies in the Southern Ocean (MESO) project. *Journal of Physical Oceanography*, *36*(12), 2232–2252. https://doi.org/10.1175/JPO2980.1

Hausmann, U., Czaja, A., & Marshall, J. C. (2016). Estimates of air-sea feedbacks on sea surface temperature anomalies in the Southern Ocean. *Journal of Climate*, *29*(2), 439–454. https://doi.org/10.1175/JCLI-D-15-0015.1

Hogg, A. M., & Blundell, J. R. (2006). Interdecadal variability of the Southern Ocean. *Journal of Physical Oceanography*, *36*(8), 1626–1645. https://doi.org/10.1175/JPO2934.1

Holte, J., Talley, L. D., Gilson, J., & Roemmich, D. (2017). An Argo mixed layer climatology and database. *Geophysical Research Letters*, *44*, 5618–5626. https://doi.org/10.1002/2017GL073426

Hunke, E. C., & Dukowicz, J. K. (1997). An elastic-viscous-plastic model for sea ice dynamics. *Journal of Physical Oceanography*, *27*(9), 1849–1867. https://doi.org/10.1175/1520-0485(1997)027<1849:AEVPMF>2.0.CO;2

Jones, J. M., Gille, S. T., Goosse, H., Abram, N. J., Canziani, P. O., Charman, D. J., et al. (2016). Assessing recent trends in high-latitude Southern Hemisphere surface climate. *Nature Climate Change*, *6*(10), 917–926. https://doi.org/10.1038/nclimate3103

Kara, A. B., Rochford, P. A., & Hurlburt, H. E. (2000). An optimal definition for ocean mixed layer depth. *Journal of Geophysical Research*, *105*(C7), 16,803–16,821. https://doi.org/10.1029/2000JC900072

Kinnison, D. E., Brasseur, G. P., Walters, S., Garcia, R. R., Marsh, D. R., Sassi, F., et al. (2007). Sensitivity of chemical tracers to meteorological parameters in the MOZART-3 chemical transport model. *Journal of Geophysical Research*, *112*, D20302. https://doi.org/10.1029/2006JD007879

Kostov, Y., Ferreira, D., Armour, K. C., & Marshall, J. C. (2018). Contributions of greenhouse gas forcing and the Southern Annular Mode to historical Southern Ocean surface temperature trends. *Geophysical Research Letters*, *45*, 1086–1097. https://doi.org/10.1002/2017GL074964

Kostov, Y., Marshall, J. C., Hausmann, U., Armour, K. C., Ferreira, D., & Holland, M. M. (2017). Fast and slow responses of Southern Ocean sea surface temperature to SAM in coupled climate models. *Climate Dynamics*, *48*(5-6), 1595–1609. https://doi.org/10.1007/s00382-016-3162-z

Kunz, A., Pan, L. L., Konopka, P., Kinnison, D. E., & Tilmes, S. (2011). Chemical and dynamical discontinuity at the extratropical tropopause based on START08 and WACCM analyses. *Journal of Geophysical Research*, *116*, D24302. https://doi.org/10.1029/2011JD016686

Lamarque, J. F., Emmons, L. K., Hess, P. G., Kinnison, D. E., Tilmes, S., Vitt, F., et al. (2012). CAM-chem: Description and evaluation of interactive atmospheric chemistry in the Community Earth System Model. *Geoscientific Model Development*, *5*(2), 369–411. https://doi.org/10.5194/gmd-5-369-2012

Large, W. G., McWilliams, J. C., & Doney, S. C. (1994). Oceanic vertical mixing: A review and a model with a nonlocal boundary layer parameterization. *Reviews of Geophysics*, *32*(4), 363–403. https://doi.org/10.1029/94RG01872

Large, W. G., & Pond, S. (1982). *Sensible and latent heat flux measurements over the ocean* (Vol. 12, pp. 464–482). Pond. https://doi.org/10.1175/1520-0485(1982)012<0464:SALHFM>2.0.CO;2

Large, W. G., & Yeager, S. G. (2009). The global climatology of an interannually varying air-sea flux data set. *Climate Dynamics*, *33*(2-3), 341–364. https://doi.org/10.1007/s00382-008-0441-3

Lin, S.-J. (2004). A "vertically Lagrangian" finite-volume dynamical core for global models. *Monthly Weather Review*, *132*(10), 2293–2307. https://doi.org/10.1175/1520-0493(2004)132<2293:AVLFDC>2.0.CO;2

Locarnini, R. A., Mishonov, A. V., Antonov, J. I., Boyer, T. P., Garcia, H. E., Baranova, O. K., et al. (2013). World Ocean Atlas 2013, Volume 1: Temperature (Tech. Rep.) Silver Spring, MD: NOAA.

Losch, M., Menemenlis, D., Campin, J. M., Heimbach, P., & Hill, C. (2010). On the formulation of sea-ice models. Part 1: Effects of different solver implementations and parameterizations. *Ocean Modelling*, *33*(1-2), 129–144. https://doi.org/10.1016/j.ocemod.2009.12.008

Marsh, D. R., Mills, M. J., Kinnison, D. E., Lamarque, J. F., Calvo, N., & Polvani, L. M. (2013). Climate change from 1850 to 2005 simulated in CESM1(WACCM). *Journal of Climate*, *26*(19), 7372–7391. https://doi.org/10.1175/JCLI-D-12-00558.1

Marshall, G. J. (2003). Trends in the Southern Annular Mode from observations and reanalyses. *Journal of Climate*, *16*(24), 4134–4143. https://doi.org/10.1175/1520-0442(2003)016<4134:TITSAM>2.0.CO;2

Marshall, J. C., Adcroft, A., Hill, C., Perelman, L., & Heisey, C. (1997). A finite-volume, incompressible Navier Stokes model for studies of the ocean on parallel computers. *Journal of Geophysical Research*, *102*(C3), 5753–5766. https://doi.org/10.1029/96JC02775

Marshall, J. C., Armour, K. C., Scott, J. R., Kostov, Y., Hausmann, U., Ferreira, D., et al. (2014). The ocean's role in polar climate change: Asymmetric Arctic and Antarctic responses to greenhouse gas and ozone forcing. *Philosophical Transactions of the Royal Society A: Mathematical, Physical and Engineering Sciences*, *372*(2019), 20130,040–20130,040. https://doi.org/10.1098/rsta.2013.0040

Marshall, J. C., Hill, C., Perelman, L., & Adcroft, A. (1997). Hydrostatic, quasi-hydrostatic, and nonhydrostatic ocean modeling. *Journal of Geophysical Research*, *102*(C3), 5733–5752. https://doi.org/10.1029/96JC02776

Marshall, J. C., Jones, H., & Hill, C. (1998). Efficient ocean modeling using non-hydrostatic algorithms. *Journal of Marine Systems*, *18*(1-3), 115–134. https://doi.org/10.1016/S0924-7963(98)00008-6

Marshall, J. C., & Radko, T. (2003). Residual-mean solutions for the Antarctic Circumpolar Current and its associated overturning circulation. *Journal of Physical Oceanography*, *33*(11), 2341–2354. https://doi.org/10.1175/1520-0485(2003)033<2341:RSFTAC>2.0.CO;2

Marshall, J. C., Scott, J. R., Armour, K. C., Campin, J.-M., Kelley, M., & Romanou, A. (2015). The ocean's role in the transient response of climate to abrupt greenhouse gas forcing. *Climate Dynamics*, *44*(7-8), 2287–2299. https://doi.org/10.1007/s00382-014-2308-0

Marshall, J. C., & Speer, K. (2012). Closure of the meridional overturning circulation through Southern Ocean upwelling. *Nature Geoscience*, *5*, 171–180. https://doi.org/10.1038/NGEO1391

Meredith, M. P., & Hogg, A. M. (2006). Circumpolar response of Southern Ocean eddy activity to a change in the Southern Annular Mode. *Geophysical Research Letters*, *33*, L16608. https://doi.org/10.1029/2006GL026499

Morgenstern, O., Hegglin, M., Rozanov, E., O'Connor, F., Luke Abraham, N., Akiyoshi, H., et al. (2017). Review of the global models used within phase 1 of the Chemistry-Climate Model Initiative (CCMI). *Geoscientific Model Development*, *10*(2), 639–671. https://doi.org/10.5194/gmd-10-639-2017

Munday, D. R., Johnson, H. L., & Marshall, D. P. (2013). Eddy saturation of equilibrated circumpolar currents. *Journal of Physical Oceanography*, *43*(3), 507–532. https://doi.org/10.1175/JPO-D-12-095.1

Neale, R. B., Richter, J., Park, S., Lauritzen, P. H., Vavrus, S. J., Rasch, P. J., & Zhang, M. (2013). The mean climate of the Community Atmosphere Model (CAM4) in forced SST and fully coupled experiments. *Journal of Climate*, *26*(14), 5150–5168. https://doi.org/10.1175/JCLI-D-12-00236.1

Panassa, E., Völker, C., Wolf-Gladrow, D., & Hauck, J. (2018). Drivers of interannual variability of summer mixed layer depth in the Southern Ocean between 2002 and 2011. *Journal of Geophysical Research: Oceans*, *123*, 5077–5090. https://doi.org/10.1029/2018JC013901

Polvani, L. M., Waugh, D. W., Correa, G. J. P., & Son, S.-W. (2011). Stratospheric ozone depletion: The main driver of twentieth-century atmospheric circulation changes in the Southern Hemisphere. *Journal of Climate*, *24*(3), 795–812. https://doi.org/10.1175/2010JCLI3772.1

Purich, A., Cai, W., England, M. H., & Cowan, T. (2016). Evidence for link between modelled trends in Antarctic sea ice and underestimated westerly wind changes. *Nature Communications*, *7*, 10409. https://doi.org/10.1038/ncomms10409

Redi, M. H. (1982). Oceanic isopycnal mixing by coordinate rotation. *Journal of Physical Oceanography*, *12*(10), 1154–1158. https://doi.org/10.1175/1520-0485(1982)012<1154:OIMBCR>2.0.CO;2

Reynolds, R. W., Rayner, N. A., Smith, T. M., Stokes, D. C., & Wang, W. (2002). An improved in situ and satellite SST analysis for climate. *Journal of Climate*, *15*(13), 1609–1625. https://doi.org/10.1175/1520-0442(2002)015<1609:AIISAS>2.0.CO;2

Rienecker, M. M., Suarez, M. J., Gelaro, R., Todling, R., Bacmeister, J., Liu, E., et al. (2011). MERRA: NASA's Modern-Era Retrospective Analysis for Research and Applications. *Journal of Climate*, *24*(14), 3624–3648. https://doi.org/10.1175/JCLI-D-11-00015.1

Roemmich, D., & Gilson, J. (2009). The 2004–2008 mean and annual cycle of temperature, salinity, and steric height in the global ocean from the Argo Program. *Progress in Oceanography*, *82*(2), 81–100. https://doi.org/10.1016/j.pocean.2009.03.004

Schmidt, G. A., Kelley, M., Nazarenko, L., Ruedy, R., Russell, G. L., Aleinov, I., et al. (2014). Configuration and assessment of the GISS ModelE2 contributions to the CMIP5 archive. *Journal of Advances in Modeling Earth Systems*, *6*, 141–184. https://doi.org/10.1002/2013MS000265

Screen, J. A., Gillet, N. P., Stevens, D. P., Marshall, G. J., & Roscoe, H. K. (2009). The role of eddies in the Southern Ocean temperature response to the southern annular mode. *Journal of Climate*, *22*(3), 806–818. https://doi.org/10.1175/2008JCLI2416.1

Seviour, W. J. M., Gnanadesikan, A., & Waugh, D. W. (2016). The transient response of the Southern Ocean to stratospheric ozone depletion. *Journal of Climate*, *29*(20), 7383–7396. https://doi.org/10.1175/JCLI-D-16-0198.1

Seviour, W. J., Gnanadesikan, A., Waugh, D., & Pradal, M. A. (2017). Transient response of the Southern Ocean to changing ozone: Regional responses and physical mechanisms. *Journal of Climate*, *30*(7), 2463–2480. https://doi.org/10.1175/JCLI-D-16-0474.1

Seviour, W. J., Waugh, D. W., Polvani, L. M., Correa, G. J., & Garfinkel, C. I. (2017). Robustness of the simulated tropospheric response to ozone depletion. *Journal of Climate*, *30*(7), 2577–2585. https://doi.org/10.1175/JCLI-D-16-0817.1

Sigmond, M., & Fyfe, J. C. (2010). Has the ozone hole contributed to increased Antarctic sea ice extent? *Geophysical Research Letters*, *37*, L18502. https://doi.org/10.1029/2010GL044301

Sigmond, M., & Fyfe, J. C. (2013). The Antarctic sea ice response to the ozone hole in climate models. *Journal of Climate*, *27*, 1336–1342. https://doi.org/10.1175/JCLI-D-13-00590.1

Sinha, A., & Abernathey, R. P. (2016). Time scales of Southern Ocean eddy equilibration. *Journal of Physical Oceanography*, *46*(9), 2785–2805. https://doi.org/10.1175/JPO-D-16-0041.1

Solomon, S., Kinnison, D., Bandoro, J., & Garcia, R. (2015). Simulation of polar ozone depletion: An update. *Journal of Geophysical Research: Atmospheres*, *120*, 7958–7974. https://doi.org/10.1002/2015JD023365

Spence, P., Saenko, O. A., Dufour, C. O., Le Sommer, J., & England, M. H. (2012). Mechanisms maintaining Southern Ocean meridional heat transport under projected wind forcing. *Journal of Physical Oceanography*, *42*(11), 1923–1931. https://doi.org/10.1175/JPO-D-12-03.1

Tamsitt, V., Drake, H. F., Morrison, A. K., Talley, L. D., Dufour, C. O., Gray, A. R., et al. (2017). Spiraling pathways of global deep waters to the surface of the Southern Ocean. *Nature Communications*, *8*(1), 1–10. https://doi.org/10.1038/s41467-017-00197-0

Tansley, C. E., & Marshall, D. P. (2001). On the dynamics of wind-driven circumpolar currents. *Journal of Physical Oceanography*, *31*(11), 3258–3273. https://doi.org/10.1175/1520-0485(2001)031<3258:OTDOWD>2.0.CO;2

Tilmes, S., Lamarque, J. F., Emmons, L. K., Kinnison, D. E., Marsh, D., Garcia, R. R., et al. (2016). Representation of the Community Earth System Model (CESM1) CAM4-chem within the Chemistry-Climate Model Initiative (CCMI). *Geoscientific Model Development*, *9*(5), 1853–1890. https://doi.org/10.5194/gmd-9-1853-2016

Viebahn, J., & Eden, C. (2010). Towards the impact of eddies on the response of the Southern Ocean to climate change. *Ocean Modelling*, *34*(3-4), 150–165. https://doi.org/10.1016/j.ocemod.2010.05.005

Viebahn, J., & Eden, C. (2012). Standing eddies in the meridional overturning circulation. *Journal of Physical Oceanography*, *42*(9), 1486–1508. https://doi.org/10.1175/JPO-D-11-087.1

Visbeck, M., Marshall, J. C., Haine, T., & Spall, M. (1997). Specification of eddy transfer coefficients in coarse-resolution ocean circulation models. *Journal of Physical Oceanography*, *27*(3), 381–402. https://doi.org/10.1175/1520-0485(1997)027<0381:SOETCI>2.0.CO;2

Winton, M. (2000). A reformulated three-layer sea ice model. *Journal of Atmospheric and Oceanic Technology*, *17*(4), 525–531. https://doi.org/10.1175/1520-0426(2000)017<0525:ARTLSI>2.0.CO;2

Zika, J. D., Le Sommer, J., Dufour, C. O., Molines, J.-M., Barnier, B., Brasseur, P., et al. (2013). Vertical eddy fluxes in the Southern Ocean. *Journal of Physical Oceanography*, *43*(5), 941–955. https://doi.org/10.1175/JPO-D-12-0178.1

Zweng, M. M., Reagan, J. R., Antonov, J. I., Locarnini, R. A., Mishonov, A. V., Boyer, T. P., et al. (2013). World Ocean Atlas 2013, Volume 2: Salinity. In S. Levitus & A. Mishonov (Eds.), *NOAA Atlas NESDIS 74* (39 pp.). Retrieved from https://data.nodc.noaa.gov/woa/WOA13/DOC/woa13_vol2.pdf